



Production of hydrochar from the hydrothermal carbonisation of food waste feedstock for use as an adsorbent in removal of heavy metals from water

Danai Pasipanodya¹ · Naadhira Seedat¹ · Bilal Patel² · Rishen Roopchand¹

Received: 12 April 2024 / Revised: 4 August 2024 / Accepted: 26 August 2024
© The Author(s) 2024

Abstract

In this research, discarded butternut peels were converted into hydrochar products through hydrothermal carbonisation (HTC), with adjustments made to the temperature (ranging from 180 to 260°C) and residence time (spanning 45–180 min). The findings indicated that both the temperature and time of carbonisation significantly influenced the yield of hydrochar (HC), as well as its physicochemical and structural properties. Higher temperatures and prolonged residence time led to decreased yield, elevated fixed carbon content and an increased fuel ratio. Furthermore, raising the process conditions increased HHV and reduced the oxygen-containing functional groups. The HC yield dropped from 28.75 to 17.58% with increased carbonisation temperature and time. The findings of this study also suggest that modified hydrochar is a promising material for removing heavy metals from wastewater. It is a relatively low-cost and abundant material that can be produced from various biomass feedstocks, including food waste. In addition, it is a sustainable and environmentally friendly option for wastewater treatment. Hydrochar-based systems offer several advantages over traditional methods of heavy metal removal, such as chemical precipitation and ion exchange. The unique physicochemical characteristics of hydrochar, including its porous structure and oxygen-rich functional groups, offer a high surface area and more binding sites for heavy metal ions. By changing the physicochemical properties of hydrochar with chemicals like phosphoric acid, it is possible to increase its adsorption capacity. The Freundlich isotherm was the best fit for the adsorption data for all three metal ions (Pb^{2+} , Cu^{2+} and Cd^{2+}), indicating that the adsorption process is multilayer and heterogeneous.

Keywords Food waste · Activated hydrochar · Hydrothermal carbonisation · Wastewater treatment · Heavy metal removal

1 Introduction

Rapid urbanisation and population growth have caused a surge in the production of municipal solid waste (MSW) worldwide, making sustainable development difficult [1]. In South Africa, particularly Johannesburg, MSW generation is particularly severe due to rapid urbanisation [2]. This escalating crisis has drawn the attention of policymakers and stakeholders at both local and international levels,

raising concerns about the growing amounts of MSW and its detrimental impacts on public health and the environment [2]. Notably, the growing organic portion of MSW, which includes food and green waste, poses a severe problem due to inappropriate disposal methods which pollute the environment, emit foul odours and release greenhouse gases into the atmosphere [3]. This negatively affects the environment, the economy and society (food insecurity). The global issue of food waste (FW) generation necessitates efficient and sustainable waste management practices. Various methods for food waste reduction and valorisation opportunities have been explored, including anaerobic digestion, composting, landfilling and thermal technologies [4]. While anaerobic digestion effectively generates fuel gas and digestate, its drawbacks include high financial investments, potential environmental impact, and operational challenges [5]. Composting, a natural process producing compost, demands a significant land area and entails costly transportation and

✉ Naadhira Seedat
naadhira@uj.ac.za

¹ Department of Chemical Engineering, Doornfontein Campus, University of Johannesburg, Johannesburg 2094, South Africa

² Department of Chemical Engineering, Florida Campus, University of South Africa, Johannesburg 1709, South Africa

handling of the moist product. Landfilling, though cost-effective, presents environmental concerns such as harmful emissions and leachate. Leveraging the abundant residual biomass in FW through thermochemical technologies to produce energy-dense biofuels and carbon-based materials can aid in establishing a circular economy and curbing waste while fostering responsible consumption and production [4].

Simultaneously, the escalating concerns over water scarcity and quality underscore the imperative for sustainable water treatment technologies. Approximately one-third of all the drinking water available globally is sourced from rivers and lakes [6]. Unfortunately, these water sources are also recipients of industrial and domestic waste, which pollutes and contaminates them with various toxins. This situation is especially evident in several African countries, including South Africa, where communities often lack access to clean water and are susceptible to waterborne diseases [7]. Wastewater contains a wide range of hazardous compounds released into the environment, endangering the environment and upsetting the natural equilibrium [8]. The natural breakdown of wastewater contaminated with heavy metals cannot occur since it would harm human tissue and organs [9]. Three methods are used to remove heavy metals from wastewater: adsorption, barrier separation and precipitation [10]. The popular and effective technique for treating wastewater containing heavy metals is adsorption technology [11]. Activated carbon and other biosorbents are often used adsorbents in the purification of wastewater. Unfortunately, the applicability of these adsorbents is limited by their high cost and the fact that they cannot be reused. Finding a low-cost, effective adsorbent to remove heavy metals from wastewater is vital to control environmental concerns [12]. One type of renewable resource that can be utilised as a feedstock to create an affordable, sustainable adsorbent is biomass waste.

Thermochemical conversion involves breaking down organic materials into solid char, liquid bio-oil and gaseous syngas facilitated by incineration, combustion, pyrolysis, gasification, torrefaction and hydrothermal carbonisation [13]. Hydrothermal carbonisation (HTC) has gained prominence as a thermal conversion method, particularly for moisture-rich wastes. HTC does not require pre-drying of feedstock, which can help conserve time and energy. First experimented in 1913, HTC utilises low temperatures, typically between 180 and 260 °C and autogenous pressures to convert food waste into energy-rich hydrochar [14, 15]. HTC mimics the geological processes that occur over millennia, transforming organic matter into hydrochar in hours. The resulting hydrochar exhibits a porous structure, high carbon content and unique surface chemistry, rendering it a material of immense interest for various applications. Hydrothermal carbonisation and pyrolysis are the two most promising processes for making

adsorbents. HTC is preferred because it is a less expensive and more environmentally beneficial treatment option than pyrolysis [16]. Hydrochar, derived from the hydrothermal carbonisation of food waste, emerges as a promising candidate, presenting an opportunity to simultaneously address two critical issues of food waste management and heavy metal pollution in water [17]. HTC has been conducted on food waste containing a mixture of rice, fish, meat, dog food, eggshells and leftover food waste. These tests were conducted at operating temperatures ranging from 200 to 350°C for 0.2 to 120 h. The findings show that the HTC of FW is advantageous, leading to the generation of hydrochar with high carbon (45–93% of initial carbon) and energy contents (15–30 kJ/g dry solids) [18]. HTC has also been tested using a mixture of waste residues (chicken meat, tomato sauce, spaghetti, noodles, and green vegetables) and found a rise in megajoules per kilogram from 25.1 to 33.1 compared to incineration [19]. Similar tests employing rabbit food wastes yielded a higher heating value of 29.1 MJ/kg with a carbon content of 67.6% [20].

The unique properties of hydrochar make it an attractive candidate for heavy metal adsorption. Its porous nature provides an extensive surface area, creating binding sites for heavy metal ions [21]. Furthermore, the functional groups on the hydrochar's surface contribute to the complexation and immobilisation of heavy metals, offering a promising avenue for efficient water treatment [22]. However, the hydrochar's adsorption capability is still limited, meaning it cannot effectively treat wastewater throughout the application process. Modifications should be made to hydrochar to enhance its adsorption capabilities. Hydrochar modification aims to improve the material's physicochemical characteristics, such as surface functional groups and porosity, to boost the material's ability to adsorb specific contaminants [12]. This study aimed to produce hydrochar from hydrothermal carbonisation of food waste for use as an adsorbent to remove Pb^{2+} , Cu^{2+} and Cd^{2+} from water. The novelty of this work is that butternut peels were used as a source of biomass feedstock. Butternut peels were preferred because they are readily available in large quantities from food processing industries, grocery stores, or households. Their abundance makes them a convenient and accessible feedstock for HTC. The hydrochar products are produced at differing temperatures and retention times. This is done to understand the properties of the solid fuel prepared at different process conditions. In this study, the physiochemical properties of both the modified and unmodified hydrochar are investigated and analysed. The adsorption performance of modified hydrochar in synthetic water is also investigated. The adsorption mechanisms of Pb^{2+} , Cu^{2+} and Cd^{2+} are also explored using the Langmuir and Freundlich isotherms.

2 Materials and methods

2.1 Feedstock

The food waste (FW) used in this project was collected from Joburg Market City Deep dumpsters, South Africa's major centre for marketing fresh produce. The food waste consisted of butternut peels (BP). The butternut peels were crushed into smaller homogenous particles in a food blender. The waste was kept in the fridge at 7°C to preserve moisture before the HTC experiment.

2.2 Preparation of hydrochar

The hydrothermal carbonisation tests were conducted in a batch system. Each test was conducted in a benchtop stainless steel high-pressure reactor with a total capacity of 1000 ml and a working volume of 800 ml. The reaction temperature was varied between 180 and 260 °C, as the HTC process should be kept below the water subcritical range since ion-product reactions might impair polymer rigidity, necessitating rigorous control below this temperature [23]. The reaction residence time was varied between 45, 90, 135 and 180 min. Table 1 shows the reaction temperature and time for each hydrochar product. Forty-eight grams of the dried blend of food waste was added to the reactor for each run. De-ionised water was utilised for the HTC reaction. The water was added in a solid–liquid ratio of 1:15 to facilitate the hydrolysis of organic materials during the HTC reactions. Pure N₂ gas was used to purge any oxygen in the reaction vessel before the reaction commenced.

Following each run, the reactor was allowed to cool overnight. The gases that could not be condensed (CO₂, CO, H₂O and CH₄) were released in a fume hood. The hydrochar (HC) and liquid product were filtered using a wet-strengthened qualitative filter. The gathered hydrochar was left in the open

to air-dry for a day. Subsequently, the dried hydrochar was collected and placed in sample plastic bags for subsequent analysis. Equation (1) was then used to compute the hydrochar mass yield [24].

$$\% \text{ Yield (dry basis)} = \frac{\text{Mass of hydrochar}}{\text{Mass of feedstock}} \times 100 \quad (1)$$

2.3 Hydrochar activation

To enhance the adsorption capacity of hydrochar, phosphoric acid (H₃PO₄) was employed to activate and modify its properties. The chemical activation process with H₃PO₄ often results in activated carbons with a well-developed pore structure and high surface area; hence, it was chosen over other activation chemicals [25]. Four hydrochar samples were activated, and these were hydrochar produced at 220 °C/45 min, 220 °C/135 min, 220 °C/180 min and 260 °C/180 min. Eighty-five percent concentrate of phosphoric acid was used, and a solution was prepared with a final volume of 40 ml containing 42.5% H₃PO₄ (17 ml). This measured quantity was accurately dispensed into four clean beakers, and distilled water was added and stirred until reaching a total volume of 40 ml. Four grams of hydrochar from each experimental run was mixed with the H₃PO₄ solution. The mixture underwent a 2-h soaking period with continuous stirring, followed by transfer to the ceramic holders. Subsequently, the mixture was heated at 500 °C for 90 min for activation inside a furnace. After activation, each mixture was oven-dried overnight at 150 °C and ground into fine particles.

2.4 Surface morphology and characterisation of the feedstock, hydrochar and activated hydrochar samples

Scanning electron microscopy Scanning electron microscopy (SEM) analysis was used to investigate the hydrochar product's surface morphology. The hydrochar was coated with carbon for better adhesion and conductivity. SEM analysis was also conducted on the AHC sample. A Thermo Scientific Phenom Desktop SEM machine was utilised.

Proximate and ultimate analysis Proximate analysis, in line with ASTM D-5142 standard method, measured the moisture, ash, volatile matter (VM) and fixed carbon (FC) content in the hydrochar and feedstock. These analyses were performed using the LECO TGA 701 instrument. Also, the ultimate analysis was done using the CHNSO elemental analyser to obtain the percentage of carbon, hydrogen, nitrogen, oxygen and sulphur in the samples.

Table 1 Reaction conditions for each experimental run

Temperature (°C)	Time (min)
180	45
	90
	135
	180
220	45
	90
	135
	180
260	45
	90
	135
	180

Higher heating value Higher heating value (HHV) is a measure of the total heat energy released when a fuel is completely burned in oxygen, and it considers the heat produced by condensing the water vapour formed during combustion. HHV was conducted on the feedstock and the hydrochar product using a Leconfield bomb calorimeter. The bomb was filled with oxygen, and the sample was ignited inside the bomb. The sample burned, releasing energy that raised the temperature of the surrounding water. The resulting temperature change in the water was measured as the heat from the combustion process was transferred to the calorimeter.

Fourier-transform infrared spectroscopy The Fourier-transform infrared spectroscopy (FTIR) was done to identify and analyse the chemical composition of the feedstock, hydrochar and the AHC. This was done using the FTIR spectrometer supplied by Thermo Scientific. The FTIR spectrum was determined over a range of 500 to 4000 cm^{-1} .

X-Ray diffraction X-Ray diffraction (XRD) was used to determine the molecular structure of the hydrochar products. Information about the arrangement of atoms or molecules within the hydrochar samples was deduced by analysing the angles and intensities of the diffracted X-rays.

2.5 Synthetic water preparation

Standard solutions of lead nitrate ($\text{Pb}(\text{NO}_3)_2$), cadmium chloride (CdCl_2) and copper sulphate (CuSO_4) were prepared by accurately weighing 1 g of each metal salts using analytical balances and dissolving them in 1 l of distilled water, separately. The pH of each metal solution was measured using a pH meter to ensure that each solution was at the optimal range for metal adsorption. The 0.1 M hydrochloric acid and 0.1 M sodium hydroxide were used to lower and raise the pH of copper sulphate and cadmium chloride solutions, respectively.

2.6 Batch adsorption test

One gram of each modified hydrochar sample was added to each metal solution in separate Erlenmeyer flasks. The flasks were placed in a thermometric shaker and agitated at 150 rpm for 4 h to enable adsorption. Each sample was then filtered to separate the solid particles of the modified hydrochar from the solution, using 45- μm vacuum filters. The metal concentrations in the filtered samples were analysed using ICP-OES supplied by Thermo Fisher Scientific. To create calibration curves for the analysis, stock solutions of lead, copper and cadmium were prepared by dissolving in distilled water and then diluted to appropriate concentrations in 50-ml capped tubes. This technique was used to detect and quantify the concentrations of the metals adsorbed,

providing accurate data on the extent of metal adsorption by the modified hydrochar.

2.7 Adsorption capacity

The metal adsorption capacity was calculated using the following equations [26]:

$$R = \frac{C_0 - C_e}{C_0} \quad (2)$$

$$q_e (\text{mg g}^{-1}) = \frac{(C_0 - C_e)V}{m} \quad (3)$$

where C_0 is the initial metal concentration (mg l^{-1}), C_e is the metal concentration at equilibrium (mg l^{-1}), V is the volume of the solution (ml), R is the adsorption efficiency, q_e is the equilibrium adsorption capacity (mg g^{-1}) and m is the amount of adsorbent used (g).

2.7.1 Isotherm models

The Langmuir and Freundlich isotherm models were used to study the equilibrium adsorption of heavy metals. The Langmuir isotherm model is given as [26]

$$q_e = \frac{Q_{\max} b_L C_e}{1 + b_L C_e} \quad (4)$$

Equilibrium parameter R_L calculated as:

$$R_L = \frac{1}{1 + b_L C_e} \quad (5)$$

where Q_{\max} (mg g^{-1}) is the maximum adsorption capacity and b_L is the Langmuir adsorption constant related to adsorption heat.

The Freundlich equation is given as:

$$q_e = K_f C_e^{1/n} \quad (6)$$

where K_f (l mg^{-1}) is the Freundlich adsorption constant and n is the heterogeneity factor.

3 Results and discussion

3.1 Proximate and ultimate analysis

The findings presented in Table 2 show the proximate analysis data on the raw butternut waste and the resultant hydrochars, indicating the physical composition of both the feedstock and the hydrochar (HC) products derived from the hydrothermal carbonisation process of the butternut waste. The moisture content in the hydrochar products exhibited a

Table 2 Proximate analysis of raw butternut waste feedstock and the hydrochars

Variation		Proximate analysis (wt.%)			
		Moisture content	Ash content	Volatile matter	Fixed carbon
Butternut peels		7.70	9.37	71.11	11.82
Hydrochar product					
HC-1	180 °C/45 min	4.79	5.62	65.05	24.54
HC-2	180 °C/90 min	4.47	6.94	69.11	19.48
HC-3	180 °C/135 min	3.35	3.66	67.94	25.05
HC-4	180 °C/180 min	3.21	2.74	68.85	15.20
HC-5	220 °C/45 min	3.09	3.62	65.85	27.44
HC-6	220 °C/90 min	2.75	3.50	64.83	28.92
HC-7	220 °C/135 min	2.67	2.42	69.86	25.05
HC-8	220 °C/180 min	2.66	2.83	55.78	39.33
HC-9	260 °C/45 min	2.03	5.73	55.92	36.32
HC-10	260 °C/90 min	2.00	4.92	55.56	37.52
HC-11	260 °C/135 min	1.98	4.01	55.03	38.98
HC-12	260 °C/180 min	2.01	3.58	54.69	39.72

notable reduction compared to that in the raw feedstock. This was a positive result since moisture reduces the energy value of the fuels, such as the hydrochar produced [27]. The raw butternut waste had a moisture content value of 7.70%. After the HTC, the moisture content of HC products decreases, ranging from 1.98 to 4.79%. Hydrochar products prepared at 260 °C experienced the most significant decrease in moisture content, with a mean moisture content of 2.01%. This was due to the high temperature of 260 °C at which these experiments were conducted. Hydrochar produced at 180 °C experienced the least decrease in moisture content with an average of 3.96%.

This decrease in moisture content can be attributed to evaporation and dewatering during the HTC experiment [28]. The FW feedstock is subjected to elevated temperatures and pressures in an aqueous environment. These conditions cause water to evaporate from the biomass. The moisture present in the biomass is effectively driven off, turning it into steam [19]. Thus, the moisture content decreases in all hydrochar products, although the hydrochar products prepared at 260 °C experienced the most significant decrease. However, it is worthy of note that the overall results indicate only a negligible difference in moisture content at high temperatures with time variations, as all the results are in the same environment of 2%, which was also observed with the other proximate parameters. The ash content represents the inorganic residue present in the feedstock. This ash content is undesirable since the combustion of materials with high ash content can lead to increased emissions of particulate matter and pollutants [3]. The butternut waste feedstock had an ash content of 9.37%. The ash content in the hydrochar products varies, ranging from 2.42 to 6.94%. HC prepared at conditions of 180 °C/180 min, 220 °C/135 min, 220 °C

/180 min and 260 °C/180 min have relatively lower ash content, suggesting effective removal of mineral matter which ended up in the liquid phase. Conversely, HC samples prepared at 180 °C/90 min and 260 °C/45 min have higher ash content. The ash content of hydrochar tends to decrease with increasing HTC temperature up to a certain point (220 °C/180 min), beyond which further increases in temperature result in increased ash content. This may indicate incomplete removal of minerals or the influence of the hydrothermal carbonisation conditions. The decrease in ash content can be attributed to the leaching of insoluble inorganic compounds, such as salts and minerals, in the biomass feedstock [29]. The feedstock is subjected to high-temperature water under pressure, which facilitates the leaching and dissolution of the soluble inorganic compounds. These soluble compounds are often water soluble and are released into the liquid phase during the HTC process [30]. As a result, they are separated from the solid hydrochar product, leading to a reduction in ash content in the hydrochar [30]. This finding contradicts what was reported by Gao et al. [31], who investigated the HTC of eucalyptus bark, resulting in the ash content increasing with an increase in residence time.

Volatile matter (VM) represents the combustible and gaseous components that can be released when the material is heated. Most biomass feedstocks have a high VM content, which is unsuitable for direct combustion due to low combustion efficiency and emission issues [32]. This investigation demonstrates that when the HTC temperature and duration increase, the VM content decreases, and the fixed carbon (FC) content increases. Fixed carbon is the carbonaceous material that remains after removing the volatile matter. The feedstock had a VM and FC content of 71.1 and 11.82%, respectively. As the HTC conditions of temperature

and time increase, the VM decreases, with HC prepared at 260 °C/90 min having the least VM at 55.56%. As the VM decreases, the FC increases, indicating an inversely proportional relationship between the two variables. The FC increases as the temperature and residence time increases. HC prepared at 260 °C/180 min had the highest FC at 39.72%, corresponding to the lowest VM. The fuel ratio (FC/VM) also increased due to the increase in temperature and reaction time. This is a good indication of whether the hydrochars obtained are intended for use as fuel. The decrease in volatile matter and increase in fixed carbon content during hydrothermal carbonisation are primarily due to the thermal decomposition of organic components, the release of volatile gases and compounds and the conversion of these volatiles into solid carbon-rich material. This transformation is desirable for producing a more stable and energy-dense carbonaceous product, which can be used for applications such as renewable energy generation, soil amendment or as a precursor for activated carbon production [23, 33].

Table 3 shows the elemental analysis of the feedstock hydrochar samples prepared at varying temperatures and times. Carbonisation of biomass involves condensation, decarboxylation and dehydration reactions that affect the oxygen, hydrogen and carbon content of the feedstock. The results highlight decreased oxygen percent at high temperatures and prolonged residence time. As temperature and time increase, the oxygen content decreases from 46.64% in the raw butternut peels to 13.81% in HC-12. This can be attributed to enhanced dehydration and decarboxylation, which leads to a drop in oxygen content. Simultaneously, an increase in carbon percent is observed with increasing temperature and time. HC-1 (180°C/45 min) has the least carbon percent at 51.29%, with HC-12 (260°C/180 min) having the

highest carbon percent at 78.73%. This finding was higher compared to the highest fixed carbon obtained by Liu et al. [28] and Saqib et al. [34] for the HTC of forest waste. The increase in carbon percent can be attributed to polymerisation and condensation secondary reactions, which occur more readily at severe reaction conditions, leading to the formation of complex carbon-rich polymers. The hydrogen percentage also decreases with increasing reaction conditions, mainly due to the increased dehydration reactions at severe reaction conditions.

3.2 High heating value

Figure 1 shows the trend in the HHV of the hydrochar products as the temperature and residence time of the experiment increase. Initially, the feedstock had an HHV value of 19.2 MJ/kg. This value increased when the feedstock underwent the HTC process at 180, 220 and 260 °C. The runs conducted at 180 °C had an average HHV of 21.975 MJ/kg. The other runs conducted at 220 and 260 °C had a mean HHV of 28.2 and 32.325 MJ/kg, respectively. The finding agrees with the study conducted by Gao et al. [31], where the HHV of the eucalyptus bark increased with an increase in temperature. This can be attributed to the removal of volatile components and oxygen at higher temperatures. Higher temperatures promote the release of volatile components, such as water vapour, carbon dioxide and small organic molecules, from the hydrochar. This process is known as devolatilisation. As these volatile components are removed, the carbon content in the hydrochar becomes more concentrated, leading to an increase in HHV [35]. Hydrothermal carbonisation becomes more efficient at converting organic matter into hydrochar at higher temperatures. This process involves breaking complex organic molecules, such as cellulose, hemicellulose and lignin, into simpler carbonaceous compounds [36]. This results in a higher carbon content in

Table 3 Elemental analysis of BP and HC on a dry basis

Variation	Ultimate analysis (wt.%)				
	C	H	O	N	
Butternut peels	43.47	6.69	46.64	3.2	
HC-1	180°C/45 min	51.29	5.83	40.09	2.79
HC-2	180°C/90 min	52.36	5.15	39.15	3.34
HC-3	180°C/135 min	58.03	5.05	34.06	2.86
HC-4	180°C/180 min	59.34	5.02	33.15	2.49
HC-5	220°C/45 min	62.85	5.13	28.95	3.07
HC-6	220°C/90 min	64.31	4.57	28.66	2.46
HC-7	220°C/135 min	66.36	4.50	26.10	3.04
HC-8	220°C/180 min	65.62	4.41	27.21	2.76
HC-9	260°C/45 min	73.75	4.59	18.7	2.96
HC-10	260°C/90 min	74.43	4.39	18.17	3.01
HC-11	260°C/135 min	77.37	4.08	15.42	3.13
HC-12	260°C/180 min	78.73	4.01	13.81	3.45

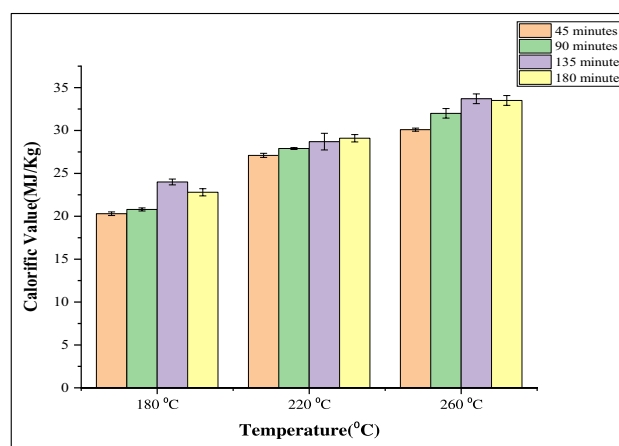


Fig. 1 Calorific values of the hydrochar products

the hydrochar, contributing to an increased HHV. At 180 °C operating temperature and 45 min of residence time, the HHV was 20.3 MJ/kg from 19.2 MJ/kg of the unprocessed feedstock. As the residence time was increased from 45 min to 90, 135 and 180 min at the same temperature of 180 °C, the HHV increased to 20.8, 24.0 and 22.8 MJ/kg, respectively. A similar trend was observed for the other two temperature conditions at 220 and 260 °C. At 220 °C, the HHV increased from 27.1 MJ/kg at 45 min to 29.1 MJ/kg at 180 min. At 260 °C, the HHV increased from 30.1 MJ/kg at 45 min to 33.5 MJ/kg at 180 min.

This was expected per a study conducted by Oktaviananda et al. [29] on the effect of residence time on the product characteristics of HTC treatment of biomass, as increased residence time leads to enhanced dehydration and deoxygenation. Dehydration removes water from the organic feedstock, reducing its moisture content and increasing the proportion of carbon in the hydrochar. Deoxygenation reactions remove oxygen-containing functional groups such as carboxyl and hydroxyl. This leads to a decreased oxygen-to-carbon ratio (O/C) and a higher HHV.

3.3 Yield

Figure 2 depicts the hydrochar yield percent at different experimental conditions. As the temperature increases from 180 to 220 °C and then to 260 °C, there is a general trend of decreasing yield. This indicates that higher temperatures lead to lower hydrochar yields. At 180 °C, the yield decreases from 28.75% at 45 min to 20.83% at 180 min. Similarly, at 220 °C, the yield decreases from 24.67% at 45 min to 19.25% at 180 min. At 260 °C, the yield decreases from 21.92% at 45 min to 17.58% at 180 min. The time

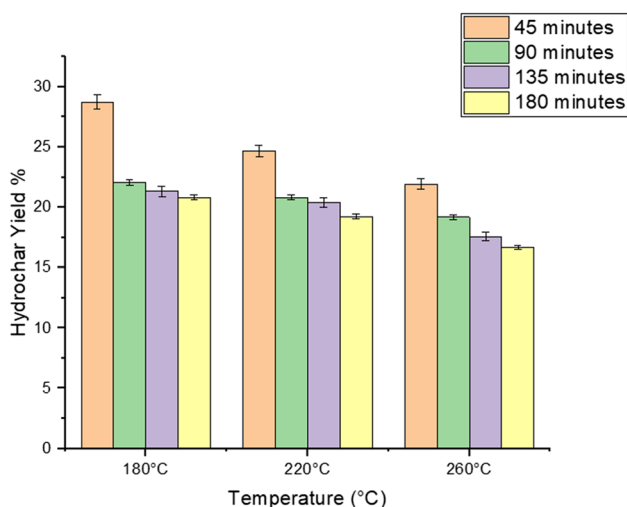


Fig. 2 Hydrochar yields at different temperatures and residence times

effect is observed at each temperature level: 180, 220 and 260 °C.

Generally, the yield tends to decrease as the hydrothermal carbonisation time increases. For example, at 180 °C, the yield decreases from 28.75% at 45 min to 20.83% at 180 min. This suggests that the longer the butternut waste is subjected to hydrothermal carbonisation, the lower the hydrochar yield. The yield trend for hydrochar formation from butternut waste during hydrothermal carbonisation shows that temperature and duration substantially impact yield. The drop in yield as temperature rises can be ascribed to a shift in reaction pathways. At higher temperatures, the reaction kinetics favour the formation of gases such as carbon dioxide and methane over solid hydrochar formation [37]. As a result, the overall yield of hydrochar is reduced. Prolonged contact with high heat and pressures can cause organic materials in butternut waste to degrade. More organic material may be converted into soluble chemicals or gases as the reaction duration increases, resulting in a decreased yield of solid hydrochar [38]. The rate of hydrothermal carbonisation reactions can vary with temperature and time. Higher temperatures may accelerate the initial reactions, leading to faster feedstock decomposition. As the reactions progress, the yield may decrease due to the formation of volatile compounds [37]. A study conducted by Oktaviananda et al. [29] on the effects of temperature on hydrochar yield reported similar findings of a decrease in HC yield as the operating temperature and time increased.

3.4 Fourier-transform infrared spectroscopy analysis

3.4.1 FTIR analysis of hydrochar

Fourier-transform infrared spectroscopy (FTIR) analysis was performed to gain a deeper insight into the functional groups in the unprocessed butternut waste and its hydrochars. Figure 3 displays the spectrum of the unprocessed feedstock and the respective hydrochars produced under varying temperatures and exposure durations. The main characteristic peaks of the feedstock and the hydrochar samples can be observed at around 3400, 2910, 1600, 1419, 1104 and 700 cm^{-1} . The peak at 3400 cm^{-1} is assigned to the O–H group vibrations [39]. The peak at 2910 can be assigned to the presence of the aliphatic C–H group. Peaks are also observed at 1600 cm^{-1} and can be attributed to C=O stretching vibrations [19]. The peak at 1419 cm^{-1} can be assigned to the C=C groups of the aromatic compound. The hydroxyl group originating from compound alcohol can be evidenced by the C–O group at the wavelength 1104 cm^{-1} . More distinctive peaks can be observed at the wave number 700 cm^{-1} . These are attributed to the presence of the aromatic C–H group.

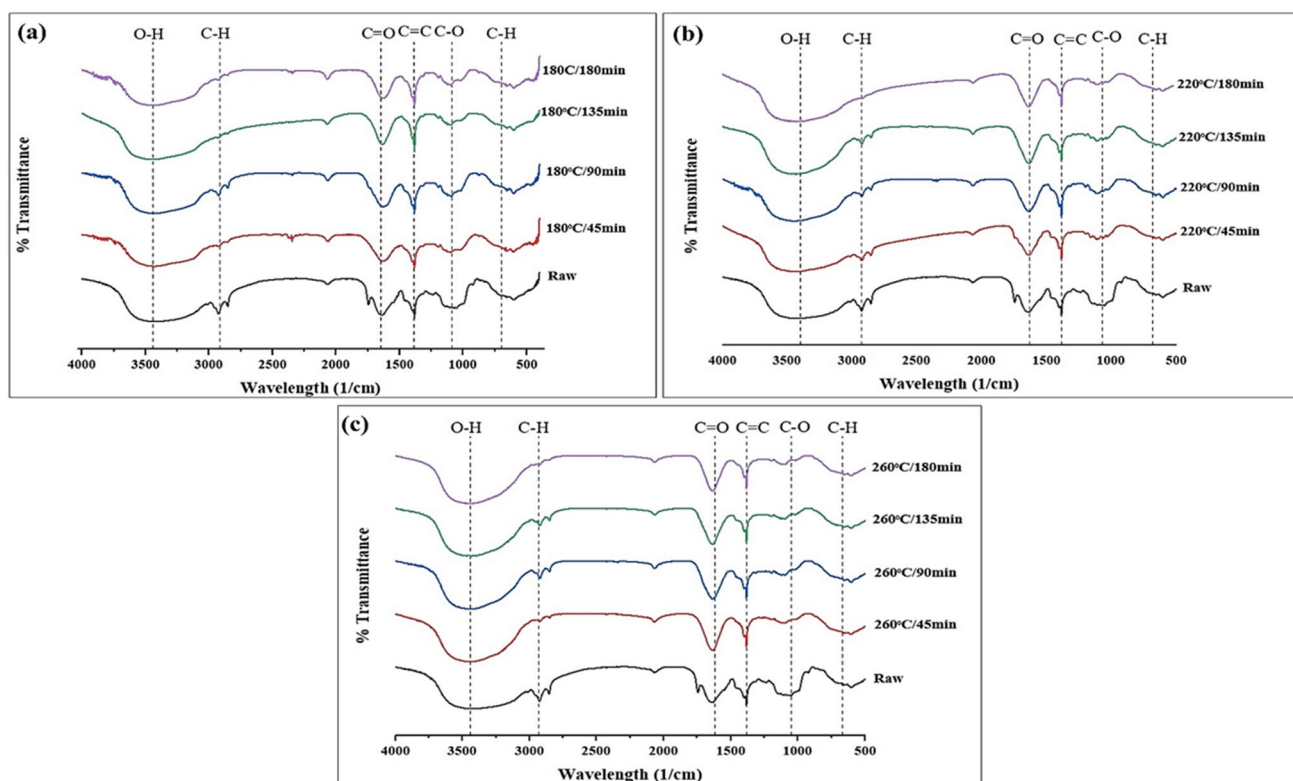


Fig. 3 FTIR spectrum of (a) hydrochar product at 180 °C, (b) hydrochar product at 220 °C, (c) hydrochar product at 260 °C in comparison with raw feed

The disappearance of the peak at 1104 cm^{-1} attributed to C–O can also be observed in all three FTIR spectra for all the hydrochar products. This results from the formation of aromatic structures during the HTC process [39]. Aromatic compounds contain fewer oxygen atoms bonded to carbon compared to the oxygen-containing functional groups in biomass. Therefore, as biomass transforms into hydrochar and forms these aromatic structures, the intensity of C–O bond signals in the FTIR spectrum decreases.

3.4.2 FTIR analysis of activated hydrochar

In the presence of phosphoric acid, a strong and broad signal associated with the stretching vibration of the hydroxyl groups at approximately 3450 cm^{-1} in all four samples was observed, as shown in Fig. 4. This indicated the presence of hydrogen-bonded hydroxyl groups from carboxyl, which appeared when the O–H groups originally in hemicellulose, cellulose, and lignin were not completely degraded during the HTC process. Bands representing the stretched vibration of C=O in carboxyl groups at about 2400 cm^{-1} were also present, conforming to the abundance of oxygen functional groups such as hydroxyl and carboxyl groups. Asymmetric and symmetric aliphatic C–H's peaks increased from 640 to 1050 cm^{-1} . The bands at 2400 cm^{-1} represented the C=O

bonds in the carboxyl and aldehyde groups. The stretching vibration peaks of C=C and C–O from the aromatic rings were at 1640 and 1390 cm^{-1} , respectively. According to a study by Ahmad et al. [40], the adsorption capacity of hydrochar for lead ions increased significantly with the increasing content of oxygen-containing functional groups. The authors attributed this enhancement to the strong electrostatic interactions between the positively charged lead ions and the negatively charged oxygen functional groups on the hydrochar surface [41]. Another study by Han et al. [42] investigated the adsorption of cadmium ions onto hydrochar prepared from sugarcane bagasse. They found that the adsorption capacity correlated highly with carboxyl and hydroxyl groups on the hydrochar surface. The authors proposed that these functional groups formed strong complexes with cadmium ions through electrostatic interactions and hydrogen bonding. Aromatic carbon structures C=C and C–O on the hydrochar surface also contribute to its adsorption capacity. Aromatic rings can provide π – π interactions with certain pollutants, leading to enhanced adsorption.

3.5 X-Ray diffraction analysis

The graphical representation of the results obtained from X-ray diffraction analysis of the hydrochar products at

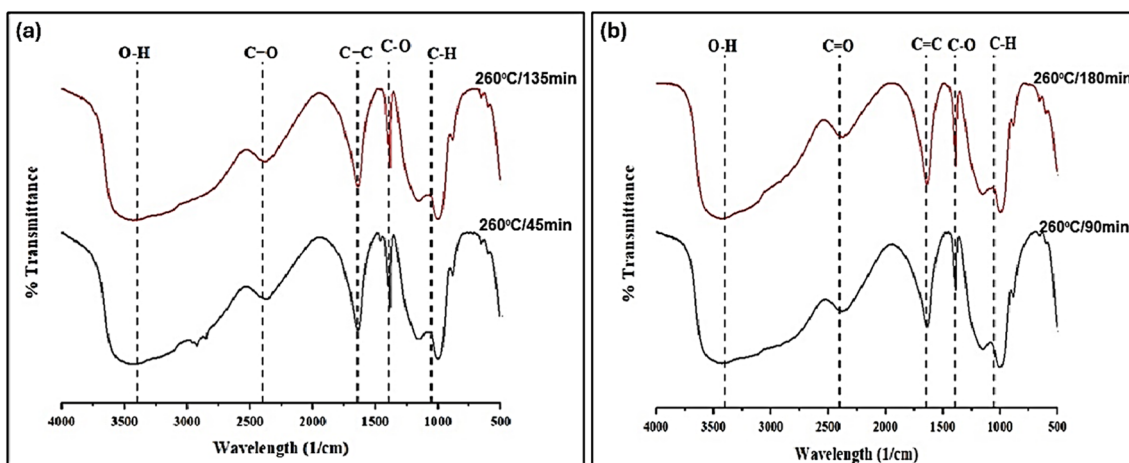


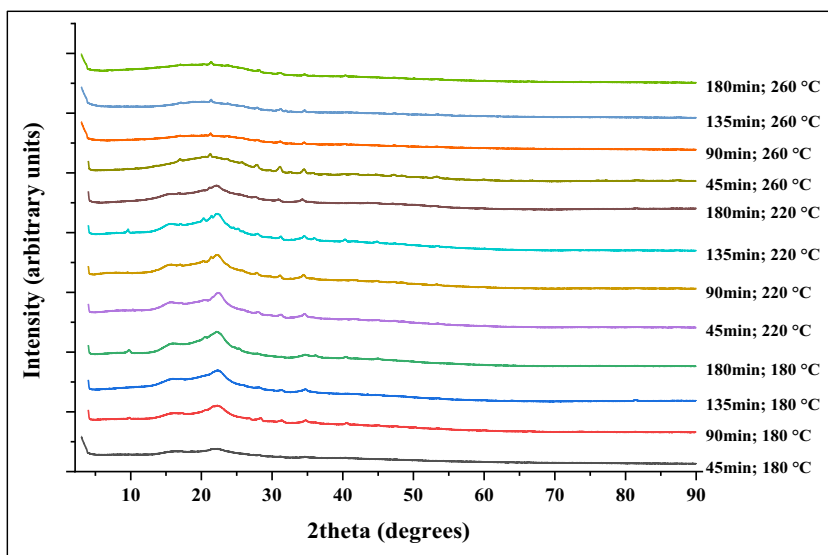
Fig. 4 FTIR spectra of (a) modified hydrochar product at 260°C and 135/45 min, (b) modified hydrochar product at 260°C and 180/90 min

different temperatures and retention times is shown in Fig. 5. The diffractogram of the hydrochar samples exhibits characteristic peaks at around $2\theta = 16, 22$ and 35° . These peaks are considered to represent cellulose [28].

Hydrochar samples obtained from lower temperatures of 180 and 220 °C clearly show the three peaks at $2\theta = 16, 22$ and 35° , indicating that the cellulose crystal structure has been preserved. With increasing temperature and time, the crystal structure gradually disappears. At 260 °C and 90 min, the curve is almost flat with no peaks. This is because high temperatures and extended reaction times can lead to increased carbonisation of the biomass and the volatilisation of volatile organic compounds. This can result in the formation of more amorphous carbon structures and a reduction in the crystallinity of the hydrochar. This phenomenon can also be seen on the two curves of

hydrochar samples prepared at 260 °C with residence times of 135 and 180 min. As the temperature increases from 180 to 220 °C, only one peak at $2\theta = 22^\circ$ can now be observed. This suggests that the crystalline structure of the cellulose is slowly being converted to an amorphous structure with increasing temperature. The crystallinity of the hydrochar samples decreased with increasing temperature. This indicated a breakdown in the hemicellulose structure’s crystalline region [43]. The maximum intensity of the peaks decreased slightly with increases in residence time compared to the changes noticed with temperature increase. The XRD patterns changed slightly with an increase in residence time due to the structural changes of the hydrochar [44]. However, the changes due to the difference in residence time were less than changes resulting from temperature difference. It can, therefore, be

Fig. 5 XRD patterns of hydrochar at different temperatures and retention times



concluded that temperature changes had a more significant impact on altering the hydrochar structure than residence time.

3.6 Scanning electron microscopy analysis

3.6.1 SEM analysis of the hydrochar sample

Figure 6 shows the SEM images of the butternut peels and the hydrochar product at different reaction conditions. The SEM images at 500 \times magnification indicate that the structure of the samples changes as the pretreatment temperature and time increase. Because of their intact state, the butternut peel samples initially possess a distinct structure with undeveloped pores (Fig. 6a). Nevertheless, the cellulosic constituent of the butternut waste samples pretreated at 180 $^{\circ}$ C had considerably disintegrated [45], resulting in the development of defined pores as seen in Fig. 6b–e, although it was not entirely transformed. This suggests that thermal decomposition may commence even at temperatures below 200 $^{\circ}$ C. As a result of the breakdown of the constituent materials during hydrothermal treatment, the smooth surfaces of raw butternut peels became rough [46]. As the temperature was increased to 220 $^{\circ}$ C, the hemicellulose structure was decomposed, creating well-developed pores. Thus, there was an increase in the microsphere structures observed at the surface of the hydrochar, which is consistent with the reported

work of Wu et al. [47]. Also, the particle size became smaller with an increase in experiment duration from 45 to 180 min for runs conducted at 220 $^{\circ}$ C since the contact time also increased, as depicted by Fig. 6f–i.

Figure 6j–m reveals that the HTC at 260 $^{\circ}$ C surface had a more obvious microsphere structure, unlike the less-defined structure in the feedstock. The formation of multiple well-developed pores is owing to the fact that samples processed via HTC at 260 $^{\circ}$ C achieved more deterioration, with big polysaccharide molecules breaking down into disaccharides and monosaccharides before being atomised into walls of carbonaceous particles [48]. The findings suggested that as the temperature and residence time increased, the initial butternut-cellulated structure gradually decomposed, transforming into smaller carbon spherical particles resulting from the decomposition of the cellulosic components during HTC [28]. It is also evident that an increase in process conditions led to the development of a more extensive network of pores within the carbonaceous material. It would be advantageous if hydrochar products were used to adsorb pollutants from wastewater [46].

3.6.2 SEM analysis of the activated hydrochar samples

Figure 7 depicts the SEM images at 1000 \times of the modified hydrochar samples after activation with phosphoric acid. The images highlight distinct differences in the surface

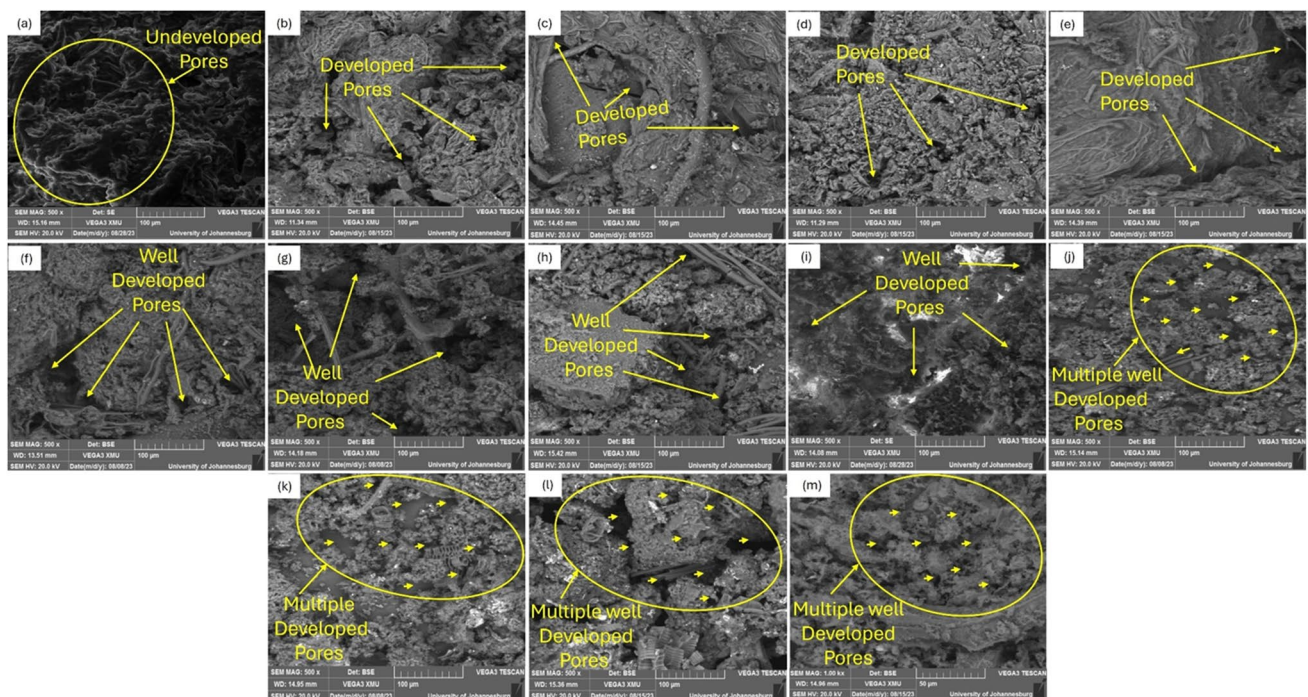
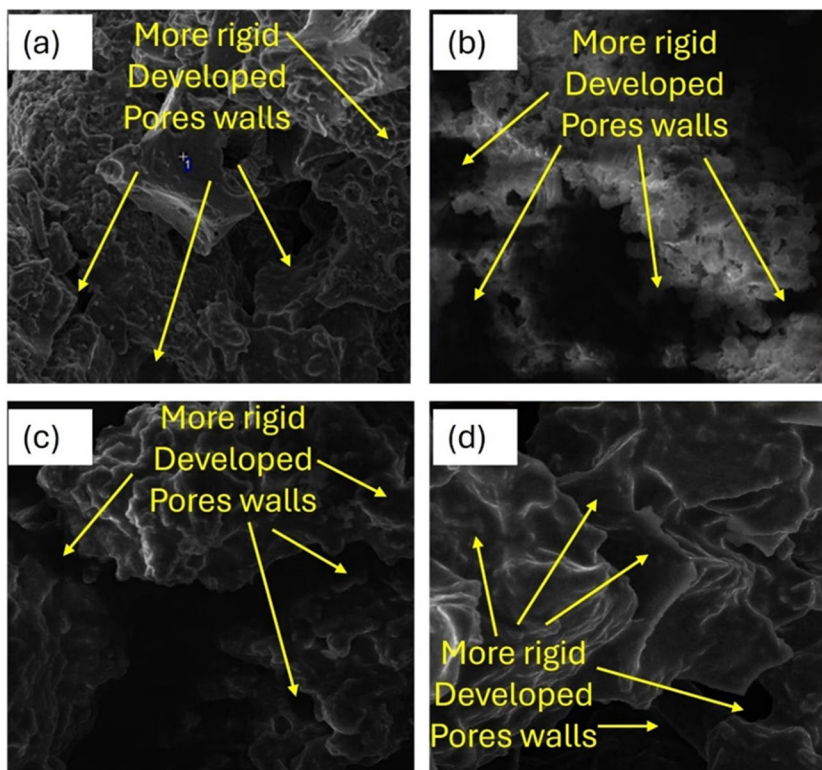


Fig. 6 SEM image of (a) raw butternut peels, (b) HC at 180 $^{\circ}$ C/45 min, (c) HC at 180 $^{\circ}$ C/90 min, (d) HC at 180 $^{\circ}$ C/135 min, (e) HC at 180 $^{\circ}$ C/180 min, (f) HC at 220 $^{\circ}$ C/45 min, (g) HC at

220 $^{\circ}$ C/90 min, (h) HC at 220 $^{\circ}$ C/135 min, (i) HC at 220 $^{\circ}$ C/180 min, (j) HC at 260 $^{\circ}$ C/45 min, (k) HC at 260 $^{\circ}$ C/90 min, (l) HC at 260 $^{\circ}$ C/135 min, (m) HC at 260 $^{\circ}$ C/180 min

Fig. 7 SEM images of modified hydrochar (a) 260 °C/45 min, (b) 260 °C/90 min, (c) 260 °C/135 min, (d) 260 °C/180 min



morphology of the samples due to the chemical and thermal modification. The activated hydrochar samples exhibited well-defined regular rigid wall structures, and texturally diverse surfaces and pores were also distributed across the surfaces of all samples. The hydrochar samples produced at 260 °C/45 min in Fig. 7a, 260 °C/90 min in Fig. 7b and 260 °C/135 min in Fig. 7c shared similar morphological characteristics with hydrochar produced at 260 °C/180 min in Fig. 7d but with fewer pores and more consistent surfaces in the later. The reduction in pores could be attributed to the collapse of wall structure from long residence high thermal treatment conditions [49]. Hence, the profile of the hydrochar sample produced at 260 °C/135 min stood out because of its pronounced rough surface and the highest number of pores observed. According to Zhang et al. [50], higher surface area and the presence of pores, cracks and channels can significantly enhance the adsorption capacity of hydrochar. Ahmad et al. also found that the surface area and pore volume of hydrochar derived from rice husk increased with increasing phosphoric acid activation. It is also known that phosphoric acid has an etching effect, which removes impurities and creates new pores in the hydrochar [40]. The presence of channels on the hydrochar surface is particularly beneficial for adsorption, as it allows for the diffusion of pollutants into the pores of the hydrochar, increasing the contact area between the pollutant and the adsorbent. Cracks on the hydrochar surface can also enhance adsorption by providing additional binding sites and increasing the surface area.

3.7 Adsorption capacity and equilibrium investigation

Adsorption is a process in which the adsorbent and adsorbate molecules interact with each other and the solvent [33]. The adsorbent–adsorbate interaction is the most crucial of the five process types that might happen during adsorption since the operation depends on it being maximised [33]. The Langmuir and Freundlich isotherm models can be used to ascertain the equilibrium characteristics of heavy metal adsorption on the adsorbent surface. The graph of $1/q_e$ versus $1/C_e$ in Fig. 8 was utilised to derive the Langmuir isotherm model. The heterogeneous or multilayer nature of the surface adsorption was ascertained using the Freundlich isotherm.

The Freundlich model was chosen as the preferred model for describing the adsorption behaviour in this study. This decision was based on comparing the Freundlich and Langmuir models' coefficient of determination (R^2) values, as depicted in the plots in Fig. 8. The R^2 values for the Freundlich model were notably higher than the Langmuir model for all three heavy metal ions (Pb^{2+} , Cu^{2+} and Cd^{2+}). Specifically, the Freundlich model obtained R^2 values of 0.9949, 0.9996 and 0.8155 for Pb^{2+} , Cu^{2+} and Cd^{2+} , respectively. In contrast, the Langmuir model yielded R^2 values of 0.9845 for Pb^{2+} , 0.9985 for Cu^{2+} and 0.616 for Cd^{2+} . Also, as shown in Table 4, the maximum adsorption capacity of each heavy metal was 332.27, 348 and 126.57 mg g^{-1} for

Fig. 8 Langmuir and Freundlich isotherm models for lead, copper and cadmium metal

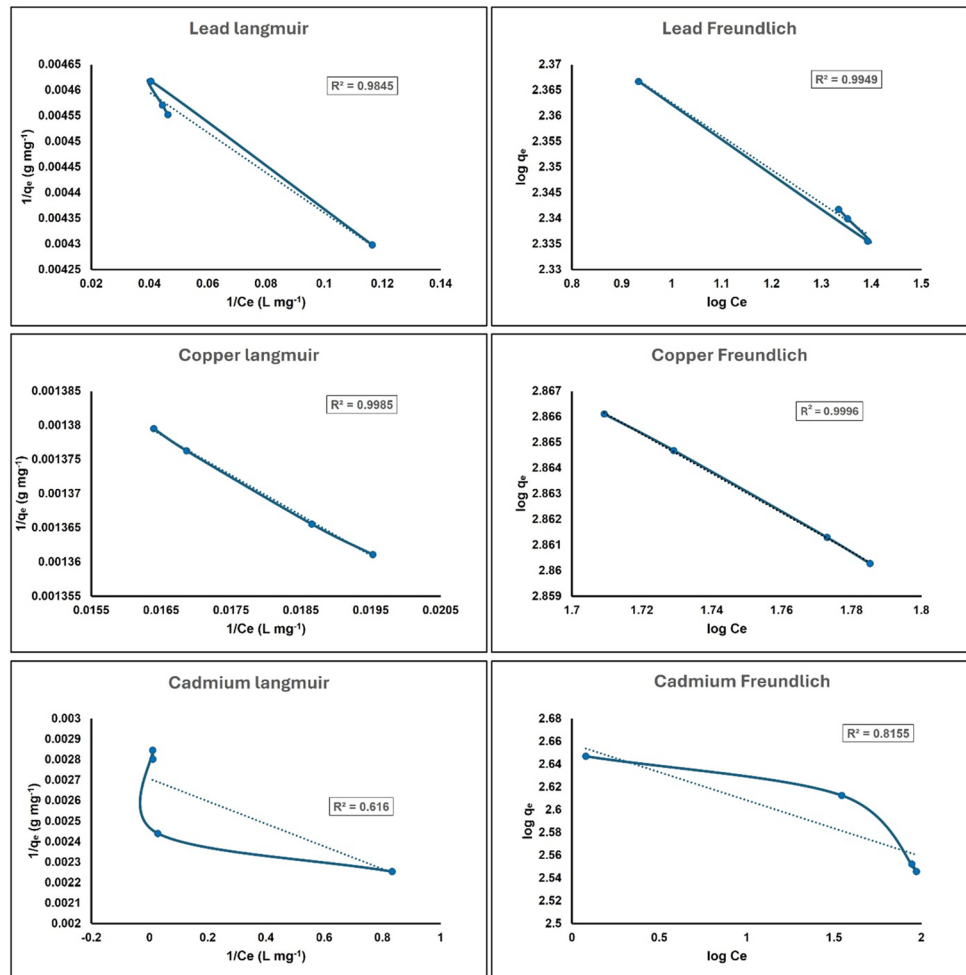


Table 4 Isotherm parameters of Pb, Cu and Cd adsorption with activated hydrochar from butternut peels

Model	Parameters	Heavy metal adsorbed		
		Pb	Cu	Cd
Langmuir	Q_e (mg g ⁻¹)	332.27	348.00	126.57
	K_L (l mg ⁻¹)	2.4480	1.4537	0.4650
	R^2	0.9845	0.9985	0.6160
Freundlich	K_F (mg g ⁻¹) (l mg ⁻¹)	386.60	240.94	117.59
	R^2	0.9949	0.9996	0.8155

lead, copper and cadmium, respectively. Compared with the study reported by Mohammed et al. [51] using nano-adsorbents, the adsorption capacity for copper and cadmium was 158 and 102.2 mg g⁻¹, respectively. This indicated a better adsorption capacity in this study; however, for lead, the adsorption capacity was 564 mg g⁻¹, which was higher than the result obtained. The higher R^2 values for the Freundlich model suggest that it provides a better fit to the experimental data for Pb²⁺, Cu²⁺ and Cd²⁺ compared to the Langmuir model in this particular study. This contrasts the

Langmuir model best fit reported for the absorption of Pb²⁺ and Cu²⁺ when rice straw was carbonised hydrothermally with and without FeCl₃ (1.2%) [16]. The Freundlich model is commonly used to describe adsorption on heterogeneous surfaces or systems involving multiple layers. The choice of the Freundlich model may imply that a heterogeneous or multilayer adsorption process more appropriately characterises the adsorption of Pb²⁺, Cu²⁺ and Cd²⁺.

4 Conclusions

This study explores butternut waste as the HTC feedstock to investigate the efficient thermochemical conversion process of FW into hydrochar. The experiments were conducted at temperatures of 180, 220 and 260 °C, and the residence time was also varied between 45, 90, 135 and 180 min to investigate the effect of changing reaction conditions on the hydrochar products. The increase in the process conditions resulted in increased fixed carbon with 78.73% as the highest obtained at 260°C/180 min while moisture content, ash content and volatile matter were reduced. The hydrochar

yield ranged from 28.57% at 180°C/45 min to 17.58% at 260°C/180 min. The highest total heat energy of 32.33 MJ/kg was obtained with the HHV analysis of hydrochar produced at 260°C/180 min, establishing suitability as a solid fuel. From the FTIR analysis, using phosphoric acid for chemical modification enhanced the oxygen-containing functional groups, increasing hydrochar's adsorptive qualities. The XRD and SEM analysis revealed that temperature and residence time significantly impacted hydrochar by increasing their micropores and regular structures. However, at 260°C/180 min, reduced numbers of pores were observed in the microstructure, as shown by the morphology. Heavy metal pollution of water is a major environmental concern. Hydrochar is an effective adsorbent for heavy metal removal from wastewater. However, the adsorption capacity of unmodified hydrochar is limited. Consequently, this study used phosphoric acid to modify hydrochar from food waste to enhance its adsorption capacity for heavy metals (Pb^{2+} , Cu^{2+} and Cd^{2+}). The adsorption capacity of the modified hydrochar for Pb^{2+} , Cu^{2+} and Cd^{2+} ions were 332.27, 348.0 and 126.57 mg g^{-1} , respectively, establishing good adsorption applicability of the produced hydrochar. Two adsorption isotherms, the Langmuir and Freundlich isotherms, were used to evaluate the adsorption capacity of the modified hydrochar. The Freundlich model obtained R^2 values of 0.9949, 0.9996 and 0.8155 for Pb^{2+} , Cu^{2+} and Cd^{2+} , respectively, while the Langmuir model yielded R^2 values of 0.9845 for Pb^{2+} , 0.9985 for Cu^{2+} and 0.616 for Cd^{2+} . The higher R^2 values for the Freundlich model showed that it provides a better fit to the experimental data compared to the Langmuir model, suggesting that the adsorption was heterogeneous and multilayer in this particular study. Thus, further investigation into the influence of adsorption parameters and established process optimisation would facilitate the consumption of HC produced from waste butternut, following its good performance in the adsorption of heavy metals.

Acknowledgements The authors thank the University of Johannesburg for the facilities in which the study was conducted.

Author contribution Naadhira Seedat: conceptualisation, supervision, investigation, visualisation, project administration, funding acquisition, writing—reviewing and editing. Danai Pasipanodya: methodology, investigation, formal analysis, validation, writing—original and final draft. Bila Patel: conceptualisation, supervision, writing—reviewing and editing. Rishen Roopchand: writing—reviewing and editing.

Funding Open access funding provided by University of Johannesburg. This project was funded by the National Research Foundation of South Africa Thuthuka Fund (Grant number: TTK220328992).

Data availability The datasets generated and analysed during the study are not publicly available due to individual privacy concerns but are available from the corresponding author on reasonable request.

Declarations

Conflict of interest The authors declare no competing interests.

Open Access This article is licensed under a Creative Commons Attribution 4.0 International License, which permits use, sharing, adaptation, distribution and reproduction in any medium or format, as long as you give appropriate credit to the original author(s) and the source, provide a link to the Creative Commons licence, and indicate if changes were made. The images or other third party material in this article are included in the article's Creative Commons licence, unless indicated otherwise in a credit line to the material. If material is not included in the article's Creative Commons licence and your intended use is not permitted by statutory regulation or exceeds the permitted use, you will need to obtain permission directly from the copyright holder. To view a copy of this licence, visit <http://creativecommons.org/licenses/by/4.0/>.

References

- Jia Y, Li H, He X, Li P, Wang Z (2023) Effect of biochar from municipal solid waste on mechanical and freeze–thaw properties of concrete. *Constr Build Mater* 368:130374. <https://doi.org/10.1016/J.CONBUILDMAT.2023.130374>
- Ayeleru OO, Fajimi LI, Oboirien BO, Olubambi PA (2021) Forecasting municipal solid waste quantity using artificial neural network and supported vector machine techniques: a case study of Johannesburg. *South Africa J Clean Prod* 289:125671. <https://doi.org/10.1016/J.JCLEPRO.2020.125671>
- Sharma HB, Dubey BK (2020) Co-hydrothermal carbonisation of food waste with yard waste for solid biofuel production: hydrochar characterisation and its pelletisation. *Waste Manage* 118:521–533. <https://doi.org/10.1016/j.wasman.2020.09.009>
- Elkhalifa S, Al-Ansari T, Mackey HR, McKay G (2019) Food waste to biochars through pyrolysis: a review. *Resour Conserv Recycl* 144:310–320
- Molino A, Chianese S, Musmarra D (2016) Biomass gasification technology: the state of the art overview. *J Energy Chem* 25:10–25. <https://doi.org/10.1016/J.JECHEM.2015.11.005>
- Mehmood MA, Qadri H, Bhat RA, Rashid A, Ganie SA, Dar GH, Shafiq-ur-Rehman (2019) Heavy metal contamination in two commercial fish species of a trans-Himalayan freshwater ecosystem. *Environ Monit Assess* 191. <https://doi.org/10.1007/s10661-019-7245-2>
- Edokpayi JN, Enitan-Folami AM, Adeeyo AO, Durowoju OS, Jegede AO, Odiyo JO (2020) Recent trends and national policies for water provision and wastewater treatment in South Africa. In: *Water conservation and wastewater treatment in BRICS nations: technologies, challenges, strategies and policies*. Elsevier, pp 187–211
- Bădescu IS, Bulgariu D, Ahmad I, Bulgariu L (2018) Valorisation possibilities of exhausted biosorbents loaded with metal ions – a review. *J Environ Manage* 224:288–297. <https://doi.org/10.1016/J.JENVMAN.2018.07.066>
- Nosuhi M, Nezamzadeh-Ejehieh A (2017) High catalytic activity of Fe(II)-clinoptilolite nanoparticles for indirect voltammetric determination of dichromate: experimental design by response surface methodology (RSM). *Electrochim Acta* 223:47–62. <https://doi.org/10.1016/J.ELECTACTA.2016.12.011>
- Zhu S, Chen Y, Khan MA, Xu H, Wang F, Xia M (2022) In-depth study of heavy metal removal by an etidronic acid-functionalized layered double hydroxide. *ACS Appl Mater Interfaces* 14:7450–7463. https://doi.org/10.1021/ACSAMI.1C22035/SUPPL_FILE/AMIC22035_SI_001.PDF

11. Lam SS, Yek PNY, Ok YS, Chong CC, Liew RK, Tsang DCW, Park YK, Liu Z, Wong CS, Peng W (2020) Engineering pyrolysis biochar via single-step microwave steam activation for hazardous landfill leachate treatment. *J Hazard Mater* 390:121649. <https://doi.org/10.1016/J.JHAZMAT.2019.121649>
12. Qin X, Meng W, Cheng S, Xing B, Shi C, Nie Y, Wang Q, Xia H (2023) Efficient removal of heavy metal and antibiotics from wastewater by phosphate-modified hydrochar. *Chemosphere* 345. <https://doi.org/10.1016/j.chemosphere.2023.140484>
13. Uma Rani R, Adish Kumar S, Kaliappan S, Yeom IT, Rajesh Banu J (2012) Low temperature thermo-chemical pretreatment of dairy waste activated sludge for anaerobic digestion process. *Bioresour Technol* 103:415–424. <https://doi.org/10.1016/J.BIORT.2011.09.124>
14. Libra JA, Ro KS, Kammann C, Funke A, Berge ND, Neubauer Y, Titirici MM, Fühner C, Bens O, Kern J, Emmerich KH (2014) Hydrothermal carbonisation of biomass residuals: a comparative review of the chemistry, processes and applications of wet and dry pyrolysis. 2:71–106. 10.4155/bfs1081
15. Gupta D, Mahajani SM, Garg A (2019) Effect of hydrothermal carbonisation as pretreatment on energy recovery from food and paper wastes. *Bioresour Technol* 285. <https://doi.org/10.1016/j.biortech.2019.121329>
16. Nadarajah K, Bandala ER, Zhang Z, Mundree S, Goonetilleke A (2021) Removal of heavy metals from water using engineered hydrochar: kinetics and mechanistic approach. *J Water Process Eng* 40. <https://doi.org/10.1016/j.jwpe.2021.101929>
17. Lin W, Murphy CJ (2017) A demonstration of Le Chatelier's principle on the nanoscale. <https://doi.org/10.1021/acscentsci.7b00302>
18. Liu Z, Quek A, Kent Hoekman S, Srinivasan MP, Balasubramanian R (2012) Thermogravimetric investigation of hydrochar-lignite co-combustion. *Bioresour Technol* 123:646–652. <https://doi.org/10.1016/J.BIORTECH.2012.06.063>
19. Wilk M, Śliz M, Gajek M (2021) The effects of hydrothermal carbonisation operating parameters on high-value hydrochar derived from beet pulp. *Renew Energy* 177:216–228. <https://doi.org/10.1016/j.renene.2021.05.112>
20. Volpe R, Messineo A, Millan M, Volpe M, Kandiyoti R (2015) Assessment of olive wastes as energy source: pyrolysis, torrefaction and the key role of H loss in thermal breakdown. *Energy* 82:119–127. <https://doi.org/10.1016/J.ENERGY.2015.01.011>
21. Rodriguez JJ, Ipiates RP, de la Rubia MA, Diaz E, Mohedano AF (2021) Integration of hydrothermal carbonisation and anaerobic digestion for energy recovery of biomass waste: an overview. *Energy Fuels* 35:17032–17050. https://doi.org/10.1021/ACS.ENERGYFUELS.1C01681/ASSET/IMAGES/LARGE/EFIC01681_0004.JPEG
22. Boakye P, Nuagah MB, Oduro-Kwarteng S, Appiah-Effah E, Kanjua J, Antwi AB, Darkwah L, Sarkodie K, Sokama-Neuyam YA (2023) Pyrolysis of municipal food waste: a sustainable potential approach for solid food waste management and organic crop fertiliser production. *Sustain Environ* 9. <https://doi.org/10.1080/27658511.2023.2260057>
23. Wu S, Wang Q, Fang M, Wu D, Cui D, Pan S, Bai J, Xu F, Wang Z (2023) Hydrothermal carbonisation of food waste for sustainable biofuel production: advancements, challenges, and future prospects. *Sci Total Environ* 897:165327
24. Wu S, Wang Q, Cui D, Wang X, Wu D, Bai J, Xu F, Wang Z, Zhang J (2023) Analysis of fuel properties of hydrochar derived from food waste and biomass: evaluating varied mixing techniques pre/post-hydrothermal carbonisation. *J Clean Prod* 430. <https://doi.org/10.1016/j.jclepro.2023.139660>
25. Lee SY, Park SJ (2015) A review on solid adsorbents for carbon dioxide capture. *J Ind Eng Chem* 23:1–11
26. Anakhu EA, Ameh VI, Modekwe HU, Ayeleru OO, Ramatsa IM (2023) Remediation of cadmium and chromium using modified *Vitex doniana* waste plant seed's biochar in quarry site surface water. *Environ Funct Mater* 2:178–188. <https://doi.org/10.1016/j.efmat.2024.02.002>
27. Hwang IH, Aoyama H, Matsuto T, Nakagishi T, Matsuo T (2012) Recovery of solid fuel from municipal solid waste by hydrothermal treatment using subcritical water. *Waste Manage* 32:410–416. <https://doi.org/10.1016/J.WASMAN.2011.10.006>
28. Liu F, Yu R, Guo M (2017) Hydrothermal carbonisation of forestry residues: influence of reaction temperature on holocellulose-derived hydrochar properties. *J Mater Sci* 52:1736–1746. <https://doi.org/10.1007/s10853-016-0465-8>
29. Oktaviananda C, Rahmawati RF, Prasetya A, Purnomo CW, Yuliansyah AT, Cahyono RB (2017) Effect of temperature and biomass-water ratio to yield and product characteristics of hydrothermal treatment of biomass. In: *AIP Conference Proceedings*. American Institute of Physics Inc
30. Cherad R, Onwudili JA, Biller P, Williams PT, Ross AB (2015) Hydrogen production from the catalytic supercritical water gasification of process water generated from hydrothermal liquefaction of microalgae. <https://doi.org/10.1016/j.fuel.2015.10.088>
31. Gao P, Zhou Y, Meng F, Zhang Y, Liu Z, Zhang W, Xue G (2016) Preparation and characterisation of hydrochar from waste eucalyptus bark by hydrothermal carbonisation. *Energy* 97:238–245. <https://doi.org/10.1016/j.energy.2015.12.123>
32. Kim MH, Song HB, Song Y, Jeong IT, Kim JW (2013) Evaluation of food waste disposal options in terms of global warming and energy recovery: Korea. *Int J Energy Environ Eng* 4. <https://doi.org/10.1186/2251-6832-4-1>
33. Khanzada AK, Rizwan M, Al-Hazmi HE, Majtacz J, Kurniawan TA, Maĳinia J (2023) Removal of arsenic from wastewater using hydrochar prepared from red macroalgae: investigating its adsorption efficiency and mechanism. *Water (Switzerland)* 15. <https://doi.org/10.3390/w15213866>
34. Saqib NU, Oh M, Jo W, Park SK, Lee JY (2017) Conversion of dry leaves into hydrochar through hydrothermal carbonisation (HTC). *J Mater Cycles Waste Manag* 19:111–117. <https://doi.org/10.1007/s10163-015-0371-1>
35. Xiao LP, Shi ZJ, Xu F, Sun RC (2012) Hydrothermal carbonisation of lignocellulosic biomass. *Bioresour Technol* 118:619–623. <https://doi.org/10.1016/j.biortech.2012.05.060>
36. Tekin K, Karagöz S, Bektaş S (2014) A review of hydrothermal biomass processing. <https://doi.org/10.1016/j.rser.2014.07.216>
37. Boutaieb M, Román S, Ledesma B, Sabio E, Guiza M, Ouederni A (2021) Towards a more efficient hydrothermal carbonization: processing water recirculation under different conditions. *Waste Manage* 132:115–123. <https://doi.org/10.1016/J.WASMAN.2021.07.023>
38. Kumar M, Oyedun AO, Kumar A (2017) A review on the current status of various hydrothermal technologies on biomass feedstock. <https://doi.org/10.1016/j.rser.2017.05.270>
39. Arellano O, Guerra J, Hidalgo A, Flores M, Rojas D, Strubinger A (2016) Hydrothermal carbonization (HTC) of corncob and characterization of the obtained hydrochar. *Iberoamerican Conference on Advanced Oxidation Technologies-CIPOA View project*. In: *Chemical Engineering Transactions*
40. Ahmad K, Bhatti IA, Muneer M, Iqbal Z (2012) Removal of heavy metals (Zn, Cr, Pb, Cd, Cu and Fe) in aqueous media by calcium carbonate as an adsorbent
41. Ahmed MB, Zhou JL, Ngo HH, Guo W (2015) Adsorptive removal of antibiotics from water and wastewater: progress and challenges. *Sci Total Environ* 532:112–126
42. Han C, Jiao Y, Wu Q, Yang W, Yang H, Xue X (2016) Kinetics and mechanism of hexavalent chromium removal by basic oxygen

- furnace slag. *J Environ Sci (China)* 46:63–71. <https://doi.org/10.1016/j.jes.2015.09.024>
43. Zhou Y, Engler N, Nelles M (2018) Symbiotic relationship between hydrothermal carbonisation technology and anaerobic digestion for food waste in China. *Bioresour Technol* 260:404–412. <https://doi.org/10.1016/J.BIORTECH.2018.03.102>
 44. Zhang L, Wang Q, Wang B, Yang G, Lucia LA, Chen J (2015) Hydrothermal carbonisation of corncob residues for hydrochar production. *Energy Fuels* 29:872–876. <https://doi.org/10.1021/ef502462p>
 45. Ameh VI, Ayeleru OO, Nomngongo PN, Ramatsa IM (2024) Bio-oil production from waste plant seeds biomass as pyrolytic lignocellulosic feedstock and its improvement for energy potential: a review. *Waste Manag Bull* 2:32–48. <https://doi.org/10.1016/j.wmb.2024.03.002>
 46. Zhang B, Heidari M, Regmi B, Salaudeen S, Arku P, Thimmanagari M, Dutta A (2018) Hydrothermal carbonisation of fruit wastes: a promising technique for generating hydrochar. *Energies (Basel)* 11. <https://doi.org/10.3390/en11082022>
 47. Wu S, Wang Q, Wu D, Cui D, Wu C, Bai J, Xu F, Liu B, Shan Z, Zhang J (2024) Influence of temperature and process water circulation on hydrothermal carbonisation of food waste for sustainable fuel production. *J Energy Institute* 112. <https://doi.org/10.1016/j.joei.2023.101459>
 48. Wu S, Wang Q, Cui D, Sun H, Yin H, Xu F, Wang Z (2023) Evaluation of fuel properties and combustion behaviour of hydrochar derived from hydrothermal carbonisation of agricultural wastes. *J Energy Inst* 108. <https://doi.org/10.1016/j.joei.2023.101209>
 49. Esther AA, Ameh VI, Meshach AA, Oluwasegun AO (2023) Preparation and characterisation of modified biochar from Vitex doniana (black plum) seeds using chemical and thermal treatments. *Asian J Res Agric Forest* 17–27. <https://doi.org/10.9734/ajraf/2023/v9i1193>
 50. Zhang Y, Zheng Y, Yang Y, Huang J, Zimmerman AR, Chen H, Hu X, Gao B (2021) Mechanisms and adsorption capacities of hydrogen peroxide modified ball milled biochar for the removal of methylene blue from aqueous solutions. *Bioresour Technol* 337. <https://doi.org/10.1016/j.biortech.2021.125432>
 51. Mohammed T, Babeker A, Chen Q. Heavy metal removal from wastewater by adsorption with hydrochar derived from biomass: current applications and research trends. <https://doi.org/10.1007/s40726-020-00172-2/Published>

Publisher's Note Springer Nature remains neutral with regard to jurisdictional claims in published maps and institutional affiliations.